Molecular Genetics and Metabolism 127 (2019) 51–57

Contents lists available at ScienceDirect

Molecular Genetics and Metabolism

journal homepage: www.elsevier.com/locate/ymgme

Direct-infusion based metabolomics unveils biochemical profiles of inborn errors of metabolism in cerebrospinal fluid

Hanneke A. Haijes[a,b,*], Maria van der Ham[a], Johan Gerrits[a], Peter M. van Hasselt[b], Hubertus C.M.T. Prinsen[a], Monique G.M. de Sain-van der Velden[a], Nanda M. Verhoeven-Duif[a], Judith J.M. Jans[a,*]

[a] Section Metabolic Diagnostics, Department of Biomedical Genetics, Centre for Molecular Medicine, University Medical Centre Utrecht, Utrecht University, Lundlaan 6, 3584 EA Utrecht, The Netherlands

[b] Section Metabolic Diseases, Department of Child Health, Wilhelmina Children's Hospital, University Medical Centre Utrecht, Utrecht University, Lundlaan 6, 3584 EA Utrecht, The Netherlands

ARTICLE INFO

Keywords:
Metabolomics
Cerebrospinal fluid
CSF
Inborn errors of metabolism
IEM
Direct-infusion mass spectrometry
DIMS

ABSTRACT

Background: For inborn errors of metabolism (IEM), metabolomics is performed for three main purposes: 1) development of next generation metabolic screening platforms, 2) identification of new biomarkers in predefined patient cohorts and 3) for identification of new IEM. To date, plasma, urine and dried blood spots are used. We anticipate that cerebrospinal fluid (CSF) holds additional – valuable – information, especially for IEM with neurological involvement. To expand metabolomics to CSF, we here tested whether direct-infusion high-resolution mass spectrometry (DI-HRMS) based non-quantitative metabolomics could correctly capture the biochemical profile of patients with an IEM in CSF.

Methods: Eleven patient samples, harboring eight different IEM, and thirty control samples were analyzed using DI-HRMS. First we assessed whether the biochemical profile of the control samples represented the expected profile in CSF. Next, each patient sample was assigned a 'most probable diagnosis' by an investigator blinded for the known diagnoses of the patients.

Results: the biochemical profile identified using DI-HRMS in CSF samples resembled the known profile, with – among others – the highest median intensities for mass peaks annotated with glucose, lactic acid, citric acid and glutamine. Subsequent analysis of patient CSF profiles resulted in correct 'most probable diagnoses' for all eleven patients, including non-ketotic hyperglycinaemia, propionic aciduria, purine nucleoside phosphorylase deficiency, argininosuccinic aciduria, tyrosinaemia type I, hyperphenylalaninemia and hypermethioninaemia.

Conclusion: We here demonstrate that DI-HRMS based non-quantitative metabolomics accurately captures the biochemical profile of this set of patients in CSF, opening new ways for using metabolomics in CSF in the metabolic diagnostic laboratory.

1. Introduction

With unprecedented pace, metabolomics is implemented in the diagnostic laboratory. For inborn errors of metabolism (IEM), metabolomics is performed for three main purposes: 1) development of next generation metabolic screening (NGMS) platforms [7,13,19] 2) identification of new biomarkers in predefined patient cohorts [1–3,9–11,20,23,29,30], and 3) for identification of new IEM [28]. To this aim, plasma, urine and dried blood spots are generally used.

The use of cerebrospinal fluid (CSF) for metabolomics analyses is lagging behind in these developments. As CSF circulates in the subarachnoidal space, surrounding brain and spinal cord, CSF is the closest possible read-out of body fluids of metabolite concentrations in the brain. For this reason, metabolomics in CSF has been used for biomarker studies for a variety of neurodegenerative diseases and cerebral infections [4–6,12,14,16,18,24,26]. However, for IEM, metabolomics studies

Abbreviations: BCAA, branched-chain amino acids; CSF, cerebrospinal fluid; DI-HRMS, direct-infusion high-resolution mass spectrometry; HMDB, Human Metabolome Database; IEM, inborn error of metabolism; m/z, mass to charge ratio; NGMS, next generation metabolic screening

* Corresponding authors at: Section Metabolic Diagnostics, Department of Biomedical Genetics, Centre for Molecular Medicine, University Medical Centre Utrecht, Utrecht University, Lundlaan 6, 3584 EA Utrecht, The Netherlands.

E-mail address: J.J.M.Jans@umcutrecht.nl (J.J.M. Jans).

https://doi.org/10.1016/j.ymgme.2019.03.005
Received 11 January 2019; Received in revised form 11 March 2019; Accepted 14 March 2019
Available online 15 March 2019

only recently expanded to CSF. Kennedy et al. determined the molecular composition of CSF and identified the biochemical pathways represented in CSF, in order to understand the potential for untargeted screening of IEM [15]. In their study, they included one patient harboring an IEM, dihydropteridine reductase deficiency (OMIM #261630), and demonstrated that they could indeed capture the biochemical signature of this disease in CSF of this patient. They conclude that further validation will illustrate the power of this technology.

In line with Kennedy et al., we acknowledge the potential power of metabolomics in CSF. We anticipate that CSF holds additional valuable information to plasma, urine and dried blood spots, especially for IEM with neurological involvement. First of all, – if CSF is available – it could add a new level of information to NGMS. Secondly, it provides the opportunity to identify biomarkers in neurometabolic IEM, for diagnostic or prognostic purposes or for treatment follow-up. Lastly, analysis of CSF could be an additional opportunity to find a diagnosis in patients that have remained without a diagnosis so far.

Here we describe the investigation of direct-infusion based non-quantitative metabolomics as a method to correctly capture the biochemical profile of patients with an IEM in CSF.

2. Materials and methods

2.1. Sample collection and patient inclusion

We used remnant CSF samples which were initially drawn for routine metabolic diagnostics or follow-up. CSF samples were collected by lumbar puncture in a standardized procedure in which six separate fractions (0.5, 1.0, 1.0, 1.5, 1.0 and 2.0 mL) were drawn and immediately put on ice at bedside. Each fraction was protected from light and stored at −80 °C. Patients with a known IEM were included when a remnant CSF sample was available in the metabolic diagnostics laboratory of the University Medical Centre Utrecht. CSF samples visually contaminated with blood were excluded. Eleven samples from eleven patients could be included. To serve as control samples, thirty samples of individuals in whom an IEM was excluded after a thorough routine diagnostic work-up turned back negative, were selected. Different fractions were available to serve as patients and control samples (fraction I in 4/41, II in 3/41, III in 1/41, IV in 10/41, V in 4/41 and VI in 19/41 samples), with a comparable distribution over the patient and control groups. All procedures followed were in accordance with the ethical standards of the University Medical Centre Utrecht and with the Helsinki Declaration of 1975, as revised in 2000. In agreement with institutional and national legislation, all included individuals, or their legal guardians, had approved the possible use of their remnant samples for method development and validation.

2.2. Sample preparation and DI-HRMS analysis

Metabolomics analysis was performed as described in [13]. In short, samples were thawed to room temperature. 10 μL of CSF was added to 140 μL a working solution containing stable isotope-labeled compounds (sILC) achieving concentrations similar to plasma [13]. The solution was centrifuged for five minutes at 17,000*g* and 105 μL of supernatant was diluted with 45 μL 0.3% formic acid (Emsure, Darmstadt, Germany). The solution was filtered using a methanol preconditioned 96 well filter plate (Acro prep, 0.2 μm GHP, NTRL, 1 mL well; Pall Corporation, Ann Arbor, MI, USA) and a vacuum manifold. The sample filtrate was collected in a 96 well plate (Advion, Ithaca, NY, USA).

Direct-infusion high resolution mass spectrometry analysis was performed using a TriVersa NanoMate system (Advion, Ithaca, NY, USA) controlled by Chipsoft software (version 8.3.3, Advion), mounted onto the interface of a Q-Exactive Plus high-resolution mass spectrometer (Thermo Scientific™, Bremen, Germany). Samples (13 μL) were automatically aspirated sequentially into a pipette tip followed by an air gap (2 μL). For each sample, technical triplicates were analyzed, infusing each sample three times into the mass spectrometer. Pipette tips were engaged with the ESI-Chip to deliver the sample using nitrogen gas pressure at 0.5 psi and a spray voltage of 1.6 kV. For each sample new pipette tips and nozzles were used to prevent any cross-contamination or carryover. The Q-Exactive Plus high-resolution mass spectrometer was operated in positive and negative ion mode in a single run, with automatic polarity switching. There were two time segments with a total run time of 3.0 min. Scan range was 70 to 600 mass to charge ratio (m/z), resolution was set at 140,000 at $m/z = 200$ for optimal separation of m/z, automatic gain control target value was 3e6, maximum injection time was 200 ms, capillary temperature was 275 °C, sample tray was kept at 18 °C and for the S-lens RF level factor 70 was used. In the positive segment, the sodium adduct of $^{13}C_6$-Phenylalanine (m/z 194.0833) was used as a lock mass and in the negative segment $^{2}H_9$-myristoylcarnitine (m/z 381.36733) was used as lock mass.

2.3. Data processing and data analysis

Data acquisition and data processing was performed using a peak calling pipeline developed in R programming language [13]. In this pipeline, detected mass peaks were annotated by matching the m/z value of the mass peak with a range of two parts per million to monoisotopic metabolite masses present in the Human Metabolome Database (HMDB), version 3.6 [32]. According to the Metabolomics Standards Initiative, the level of certainty in metabolite identification is 2, as we putatively annotate compounds based on the matched m/z value of the mass peak (Sumner et al. 2017), Mass peak intensities of mass peaks annotated without adduct ion or with a single adduct ion in negative ($[M\text{-}H]^-$, $[M + Cl]^-$) or positive ($M + H]^+$, $[M + Na]^+$ and $[M + K]^+$) mode were summed. Hereof, annotations of metabolites that could occur endogenously and annotations of metabolites with still unknown function were manually curated by four trained clinical laboratory geneticists [13]. For each mass peak per patient sample, the deviation from the intensities in control samples was indicated by a *Z*-score, calculated by: *Z*-score = (intensity patient sample–mean intensity control samples)/standard deviation intensity control samples. For each sample, metabolite annotations were ranked on *Z*-score: positive *Z*-scores were ranked from rank 1 onwards from the highest *Z*-scores to a Z-score of 0.0, and negative Z-scores were ranked from rank (−)1 onwards from the lowest Z-scores to a Z-score of 0.0. Z-scores are considered aberrant when > 2.0 (as a Z-score of 1.96 corresponds to a *p*-value of 0.05) or < −1.5, since decreases are often more subtle than increases. Data and R code can be supplied upon request [13]. Ratios were calculated by dividing the mass peak intensities and by subsequently calculating the *Z*-scores.

2.4. Assessing the biochemical profiles of control and patient samples

To assess whether the biochemical profile of control samples identified with DI-HRMS represents the expected biochemical profile of CSF, it was determined whether metabolites that are enlisted in HMDB as “detected and quantified in CSF” were identified using our method. Next, metabolites measured with the highest median intensities in the control samples were listed. The most abundant metabolites in CSF, as described by [31], were expected to have relatively high intensities.

Next, to assess whether the patient biochemical profile identified with DI-HRMS represents the expected patient biochemical profile, each patient was assigned a ‘most probable diagnosis’ by an investigator blinded for the patient's known diagnosis. This assigned ‘most probable diagnosis’ was based on the ranked metabolite list as provided by the workflow. For all metabolite annotations with aberrant *Z*-scores (> 2.0 and < −1.5), association to any known IEM was assessed. Next, Z-scores of all annotated intermediates of the involved pathways were inquired, to confirm or confute a possible diagnosis. Neither information regarding patient characteristics (sex, age), nor clinical

information was provided to the investigator.

Per included IEM, a list was composed, comprising expected increases and decreases of metabolites, based on whether it is the substrate or product of the defective enzyme, and on reported increases or decreases in CSF, plasma, dried blood spots or urine in OMIM and additional literature [8,13,17].

3. Results

3.1. Biochemical profile of control samples

The biochemical profile of control samples identified with DI-HRMS represented the expected biochemical profile of CSF ([31], HMDB). In our peak calling pipeline, 1811 mass peaks were annotated with 3676 metabolites that could occur endogenously (Supplementary Material). The relative standard deviation of the within-run variation was 0.17, thus satisfactory. We compared our results to the metabolites enlisted as "detected and quantified in CSF" in the HMDB. This HMDB list comprises 448 metabolites, of which 70 metabolites have masses $< 70\ m/z$ or > 600 m/z and were therefore not detectable using the m/z range selected for this study. Furthermore, we classified 34/448 metabolites as exogenous metabolites and 13/448 metabolites as drug metabolites and excluded these compounds. Of the remaining 331 metabolites, our method annotated 321 (97%) metabolites to 210 mass peaks. Interestingly, our method identified 1601 additional mass peaks with endogenous metabolite identifications in CSF (Supplementary Material).

The forty mass peaks with the highest median intensities in thirty CSF control samples are shown in Fig. 1. As expected, these mass peaks include mass peaks annotated with hexoses or cyclohexanes (glucose, fructose, galactose and/or myo-inositol, #1), lactic acid (#3), citric acid (#5), glutamine (#6) and ascorbic acid (#21). More metabolites described to be abundant in CSF were annotated: creatinine (#10) and creatine (#29), pyroglutamic acid (#52), ribitol (#73), glycerol (#79), 2-hydroxybutyric acid (#85), succinic acid (#100), glutamate (#128), serine (#141) and alanine (#146) [31] (Supplementary Material).

Interesting metabolites present among the forty metabolites with the highest intensities in CSF, are metabolites of the degradation pathway of branched-chain amino acids (BCAA): senecioic acid (#8), ketoleucine (#16), 2-hydroxy-3-methylpentanoic acid (#23) and alpha-ketoisovaleric acid (#27) and the free fatty acid oxidation products trans-4,5-epoxy-2(*E*)-decenal (#2), 4-oxo-2-nonenal (#15), 4-hydroxynonenal (#26, described to be present in CSF), 4-hydroperoxy-2-nonenal (#33) and 3-(3-ethyloxiranyl)-2-propenal (#40).

3.2. Biochemical profile of patient samples

The biochemical profiles of the patient CSF samples analyzed by DI-HRMS, all showed abnormalities in line with the genetic defects of the patients. Of all eleven included patients, the 'most probable diagnoses' assigned to the patient based on the metabolomics profile was correct, including non-ketotic hyperglycinaemia, propionic aciduria, purine nucleoside phosphorylase deficiency, argininosuccinic aciduria, tyrosinaemia, non-tetrahydrobiopterin deficient hyperphenylalaninaemia and hypermethioninaemia. Fig. 2 demonstrates the *Z*-scores of a selection of relevant biomarkers on which assigned diagnoses were based, for patients compared to controls. Table 1 lists Z-scores of the most important and interesting metabolites for these IEM.

Non-ketotic hyperglycinaemia is an IEM that generally presents with severe epileptic encephalopathy and hypotonia in the neonatal period. It is due to an enzyme deficiency of the glycine cleavage system. The diagnosis is mainly based an increase of glycine in CSF. We could identify this IEM in one patient (P1), based on an isolated significant increase of glycine (Table 1, Fig. 2). Metabolites associated with diseases that also can present with an increase of glycine all had normal *Z*-scores.

We identified propionic aciduria, a deficiency of propionyl-CoA carboxylase, in one patient (P2), based on a significant increase of propionylcarnitine, 2-methylcitric acid, propionylglycine and 3-hydroxypropionic acid, which all are products of the reactive enzymatic substrate propionyl-CoA, and on a significant decrease of L-carnitine, a scavenger of propionyl-CoA (Table 1, Fig. 2). Methylmalonic acid and methylmalonylcarnitine, which are expected to be increased in methylmalonic acidemia, a closely related IEM, were both normal (*Z*-scores 0.02 and −0.51, respectively).

Purine nucleoside phosphorylase deficiency is a progressive neurological disorder which presents with spasticity, movement disorders and retardation. This IEM was identified in one patient (P3), based on the combined significant increases of inosine, one of the substrates of purine nucleoside phosphorylase (Fig. 2), and a significant decrease of uric acid, a downstream metabolite in the affected pathway (Table 1).

Argininosuccinic aciduria was identified in one patient (P4), based on a stunning increase of argininosuccinic acid, the substrate of the enzyme. Argininosuccinic acid is normally very low in CSF (mean mass peak intensity 28,857; standard deviation 2928), and was found vastly increased (mass peak intensity 4,997,820). In support, citrulline and orotidine, metabolites upstream in the affected metabolic pathway, also show a significant increase. In untreated samples, arginine (the product of the enzymatic reaction) is expected to be decreased, but due to arginine supplementation, which is the appropriate therapy for this disease, this patient demonstrates a significant increase of arginine in CSF.

Tyrosinaemia, without specifying the type of tyrosinaemia, was identified in two patients with tyrosinaemia type I (P5, P6). Tyrosinaemia type I is due to a deficiency of fumarylacetoacetase, which converts fumarylacetoacetate into fumarate and acetoacetate. The diagnosis is generally based on a significant increase of tyrosine (Table 1, Fig. 2), a metabolite upstream in this metabolic pathway. In both patients hydroxyphenyllactic acid – a tyrosine derivative – was significantly increased as well. Succinylacetone, the most toxic metabolite produced in tyrosinaemia type I, distinguishing type I from type II and III, was not increased, since both patients were treated with a tyrosine restricted diet and nitisinone at the moment of sampling. Interestingly, in one patient sample (P5), the substrate of fumarylacetoacetase was increased: 4-fumarylacetoacetic acid ranked 11th with a *Z*-score of 3.06 (Table 1), providing additional information that this patient, is, indeed, affected with tyrosinaemia type I.

Non-tetrahydrobiopterin deficient hyperphenylalaninaemia is most often caused by a deficiency of phenylalanine hydroxylase, which converts phenylalanine into tyrosine. Untreated, the disease is characterized by severe brain damage with intellectual disability, spasticity and seizures. Non-tetrahydrobiopterin deficient hyperphenylalaninaemia was identified in two patients (P7,P8), based on a significant increase of the substrate of phenylalanine hydroxylase: phenylalanine, combined with a significant increase of the substrate/product ratio: the ratio of phenylalanine over tyrosine (Table 1, Fig. 2) and normal pterines and neurotransmitters. The substrate/product ratio is very important for recognition of an IEM, as phenylalanine can also be increased due to a general surplus of amino acids. In Fig. 2 it is shown that also one control sample has a significant increase of phenylalanine (*Z*-score 3.52), but it ranks at 38 only (pointing to many increased metabolites) and the phenylalanine/tyrosine ratio is much lower than in both patients (Z-score 2.82, rank 73), making a genetic defect causing the observed hyperphenylalaninaemia in this control sample unlikely. The affected gene in P7 is *PAH*, the affected gene in P8 is *DNAJC12*.

Lastly, hypermethioninaemia, an IEM characterized by demyelination and intellectual disability, is caused by a deficiency of methionine adenosyltransferase I. This IEM was correctly identified in three patients (P9-P11), based on a significant increase of methionine, the substrate of the deficient enzyme (Table 1, Fig. 2). In two patients (P10, P11), homocysteine thiolactone was also increased, and in one patient (P11) S-adenosylmethionine, the enzymes' product, demonstrated a significant decrease (Table 1).

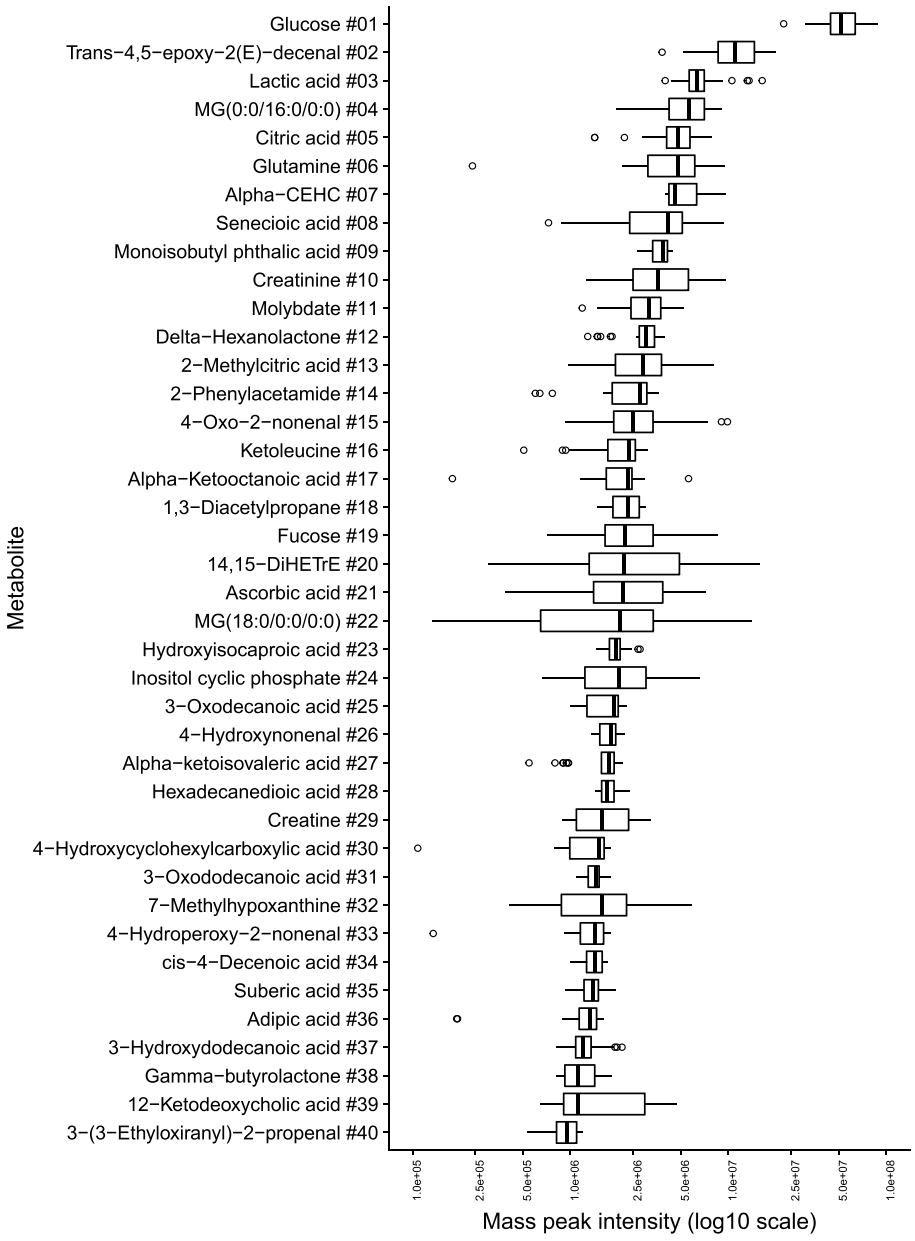

Fig. 1. Forty mass peaks with the highest median intensities in CSF control samples.
Boxplots of mass peak intensities of forty mass peaks with the highest median intensities in thirty CSF control samples. The y-axis displays the mass peaks with for each mass peak, one of the annotated metabolites. For the full list, see Supplementary Material. Mass peaks are ordered on median mass peak intensity. The x-axis displays the measured mass peak intensity on a logarithmic scale.

4. Discussion

This is the first study using DI-HRMS for non-quantitative metabolomics in CSF. The method is fast, requires only 10 µL of CSF and it correctly captures the biochemical profile of CSF in control samples. We could annotate 97% of the 331 metabolites that could occur endogenously (*m/z* 70–600) enlisted in HMDB as "detected and quantified in CSF". The unselective nature of the method even allowed for annotation of 1811 mass peaks with metabolites that could occur endogenously, with a level of certainty of 2, according to the Metabolomics Standards Initiative [27]. Among the mass peaks with the highest median intensities were, as expected, mass peaks annotated with glucose, lactic acid, citric acid, glutamine, creatinine, ascorbic acid and creatine. In addition, we observed metabolite groups that were not reported in CSF before. Interestingly, several metabolites of the BCAA degradation pathway were also among the mass peaks with the highest median intensities. Ketoleucine and 3-methyl-2-oxoisovaleric acid (#16, isomers) are the direct products of reversible transamination of leucine and isoleucine, and alpha-ketoisovaleric acid (#27) is the direct product of reversible transamination of valine. These transaminations provide nitrogen for the concurrently occurring conversion of alpha-ketoglutarate into glutamate, an important neurotransmitter in the brain. Yudkoff recently reviewed these interactions of the glutamine/glutamate cycle and the BCAA and keto acids in the central nervous system. BCAA transamination is responsible for approximately one third of glutamine synthesis, the latter part being provided by leucine [33]. The importance of this glutamate-BCAA cycle could explain the relative abundance of keto-acids in CSF.

Another set of metabolites found with relatively high median intensities were free fatty acid oxidation products as 4-hydroxy-2-nonenal. This metabolite is produced during peroxidation of omega-6-polyunsaturated fatty acids as arachidonic acid and linoleic acid [25].

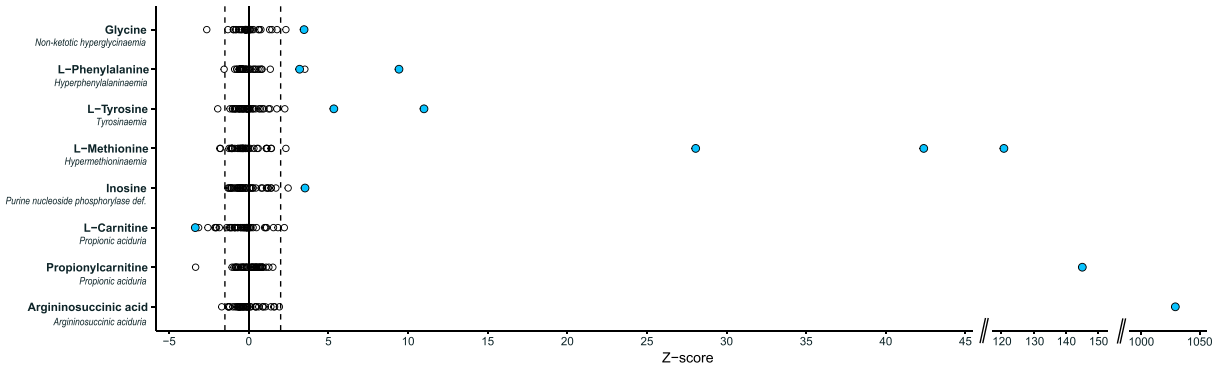

Fig. 2. Distribution of Z-scores of a selection of relevant biomarkers on which patient 'most probable diagnoses' were based.
Four amino acids and four other metabolites are demonstrated as representative examples of compounds annotated to a mass peak with increased or decreased *Z*-scores that contributed to the assigned probable diagnosis. Each dot represents a unique sample. Black open circles represent both control samples and samples of other IEM patients, blue filled circles represent patients with that specific IEM. The dashed lines depict the cut-off values for aberrant Z-scores: > 2.0 for positive values and < -1.5 for negative values. (For interpretation of the references to colour in this figure legend, the reader is referred to the web version of this article.)

It is considered to be a biomarker of lipid peroxidation in vivo [25]. Lipid peroxidation in the brain has been associated with many pathophysiological processes in a wide range of neurological disorders [25]. Therefore, the relative abundance of the free fatty acid oxidation products that we found in control samples might reflect the underlying neurological conditions in these patients that initially required additional investigations in CSF, and might not resemble the abundance of free fatty acid oxidation products of a truly healthy population.

The eight mass peaks of the HMDB list that we could not identify in this CSF series were molybdenum (*m/z* 96.9400), palladium (m/z 106.4200), triphosphate (m/z 257.9550), thiamine (m/z 265.3550), 8-isoprostane (m/z 280.5316), 7- and 8- dehydrocholesterol (m/z 384.6377), adenine diphosphate (m/z 427.2011) and guanosine diphosphate (m/z 443.2005). However, we repeatedly have identified all these mass peaks in plasma and dried blood spots (data available on request). Furthermore, in another CSF dataset we did identify palladium, triphosphate and 7- or 8-dehydrocholesterol, albeit with intensities just above the detection limit (data available on request). Thus, the reason for missing these metabolites is not in sample preparation, sample analysis or data processing, so it is most likely due to metabolite concentrations being just below the detection limit.

DI-HRMS metabolomics also correctly captured the biochemical profile of IEM patients. In all eleven included patients the known patient diagnosis was correctly identified, so we can conclude that these IEM biochemical profiles are accurately captured with our DI-HRMS workflow. However, a limitation of our study is the still limited set of patient samples and different IEM included in the study. It was not possible to test other IEM, due to limited availability of samples of – preferably untreated – patients with known IEM. We are open to receiving more samples for further validation.

We here demonstrate, that next to nuclear magnetic resonance, gas chromatography and liquid chromatography mass spectrometry [31], DI-HRMS is a suitable method to display the biochemical profile of CSF. In very limited amounts of patient material, only 10 µL, we detect > 1800 mass peaks, with metabolite concentrations ranging from millimolars for glucose (2.960 ± 1.110 mM, [31]) to nanomolars for L-cysteine (58 nM, [22]) and methylguanidine (< 50 nM, [21]). To our knowledge, mass peak identification in CSF to this extent has not been described before.

In theory, DI-HRMS based metabolomics in CSF can meet three main purposes: 1) NGMS, 2) biomarker identification and 3) identification of yet unknown IEM. A fourth potential application of CSF metabolomics is evaluation of treatment effects. We demonstrated that we captured both treatment (increase of arginine in a patient with argininosuccinic aciduria, treated with arginine) and treatment effects (normal succinylaceton in a patient with tyrosinaemia type I, treated with a tyrosine restricted diet and nitisinone). However, one should always weigh the expected benefit of this way of evaluating treatment effectiveness against the burden of a very invasive procedure, so we expect the use of CSF metabolomics for evaluation of treatment effectiveness only when specific information on the brain effect of treatment is needed. We expect that metabolomics in CSF will have most added value for NGMS, for the identification of new biomarkers and for the identification of yet unknown IEM. For the identification of biomarkers for neurometabolic IEM for which a biochemical hallmark is not yet known, CSF samples of a cohort of patients with a specific IEM could be compared to control samples. In addition, for the identification of new biomarkers for neurometabolic IEM that are – biochemically – difficult to distinguish from another IEM, cohorts of patients with these IEM can be compared. Next to diagnostic purposes, identification of new biomarkers for neurometabolic IEM could elucidate pathophysiological mechanisms in neurometabolic IEM that are not yet fully understood. To serve NGMS and the identification of yet unknown IEM, we anticipate that in patients suspected of a neurometabolic disease, metabolomics in CSF could hold additional information on increased and decreased metabolite annotations of many different metabolic pathways that might provide a diagnostic lead, for both known and yet unknown IEM. This diagnostic lead can subsequently be evaluated by targeted diagnostics, analysis of enzymatic activity and/or genetic testing. Thus, in summary, DI-HRMS metabolomics in CSF – as the closest possible read-out of body fluids of metabolite concentrations in the brain – could serve both improvements in metabolic diagnostics as well as it could provide new insights in pathophysiological mechanisms in neurometabolic IEM.

5. Conclusion

By correctly assigning a 'most probable diagnosis' to all included patients harboring an IEM, we here demonstrate that direct-infusion based non-quantitative metabolomics accurately captures the biochemical profile of patients in CSF. This opens new ways for using metabolomics in CSF for NGMS, for biomarker identification in IEM, and for finding a diagnosis in the yet undiagnosed patients suspected of a neurometabolic disease.

Funding

This work was supported by the personal Alexandre Suerman Stipend of the University Medical Centre Utrecht (H.A.H.) and by Metakids (2017-075) (J.J.M.J).

Table 1
Assigned 'most probable diagnoses' based on diagnostic metabolites in CSF.

Most probable diagnosis	Metabolite[a]	Expected change[b]	Patient	Rank	Z-score	Patient	Rank	Z-score	Patient	Rank	Z-score
Non-ketotic hyperglycinaemia (MIM #605899)	Glycine	Increase, substrate	P1	8	3.47						
Propionic aciduria (MIM #606054)	Propionylcarnitine	Increase	P2	1	144.68						
	2-Methylcitric acid	Increase		18	5.60						
	3-Hydroxypropionic acid	Increase		40	3.96						
	Propionylglycine	Increase		41	3.96						
	Heptadecanoylcarnitine	Increase [1]		63	2.70						
	Glycine	Increase		175	−0.13						
	Propionic acid	Increase		78	−1.11						
	L-Carnitine	Decrease		2	−3.36						
Purine nucleoside phosphorylase deficiency (MIM #613179)	Inosine	Increase, substrate	P3	26	3.53						
	Guanosine	Increase, substrate		146	−0.30						
	Deoxyinosine	Increase		172	0.72						
	Deoxyguanosine	Increase		175	−0.01						
	Guanine	Decrease, product		242	0.02						
	Hypoxanthine	Decrease, product		107	−0.69						
	Uric acid	Decrease		26	−1.61						
Argininosuccinic aciduria (MIM #207900)	Argininosuccinic acid	Increase, substrate	P4	1	1032.09						
	Citrulline	Increase		14	7.13						
	Orotidine	Increase		42	3.55						
	Glutamine	Increase		147	1.16						
	Uracil	Increase		178	−0.04						
	Orotic acid	Increase		77	−1.05						
	Arginine	Decrease		22	5.50						
Tyrosinaemia (type not specified)	L-Tyrosine	Increase, substrate (II)	P5	1	11.00	P6	8	5.34			
	Hydroxyphenyllactic acid	Increase		2	6.64		1	14.35			
	Hydroxyphenylacetic acid	Increase		113	−0.74		41	1.65			
Type I (MIM #276700)	4-Hydroxyphenylpyruvic acid	Increase, substrate (III)		100	−0.87		190	−0.29			
Type II (MIM #276600)		Decrease, product (II)									
Type III (MIM #276710)	5-Aminolevulinic acid	Increase		57	−1.32		194	−0.25			
	4-Fumarylacetoacetic acid	Increase, substrate (I)		11	3.06		171	−0.48			
	Succinylacetone	Increase (I)		162	0.17		154	−0.65			
	Fumaric acid	Decrease, product (I)		90	−0.97		166	0.15			
	Acetoacetic acid	Decrease, product (I)		122	−0.65		123	−0.96			
Hyperphenylalaninaemia, non-tetrahydrobiopterin deficient (genetic defect not specified)	Phenylalanine/Tyrosine ratio	Increase	P7	6	3.95	P8	9	6.76			
	L-Phenylalanine	Increase, substrate (#1)		11	3.19		6	9.43			
	Phenylpyruvic acid	Increase		171	0.19		250	0.01			
	Phenylacetic acid	Increase		118	−0.63		205	0.46			
#1 PAH (MIM #261600)	Phenyllactic acid	Increase		39	−1.47		155	−0.25			
#2 DNAJC12 (MIM #606060)	Tyrosine	Decrease, product (#1)		124	−0.57		180	0.00			
Hypermethioninaemia (MIM #250850)	Methionine	Increase, substrate	P9	1	121.94	P10	3	42.38	P11	3	28.06
	Homocysteine	Increase[2]		216	−0.06		155	−0.22		161	−0.09
	Homocysteine thiolactone	Increase[3]		89	−1.01		20	3.61		8	4.72
	S-Adenosylmethionine	Decrease, product		68	−1.24		131	0.83		8	−2.25

[a] Metabolite annotations that were expected to be increased or decreased in patient samples are reported, although more metabolite annotations have influenced the final decision. For each mass peak, only one metabolite annotation is reported, the annotation that influenced the final decision. Metabolite annotations that are not reported were either less relevant for assigning the most probable diagnosis, or were normal. All data is available on request.

[b] Expected change indicates whether a metabolite can be expected to be increased or decreased in the patient samples, based on whether it is the substrate or product of the defective enzyme, and on increases or decreases in CSF, plasma, dried blood spots or urine reported in OMIM and additional literature.

[1] **[17]**.

[2] **[8]**.

[3] **[13]**

Competing interests

All authors state that they have no competing interests to declare. None of the authors accepted any reimbursements, fees or funds from any organization that may in any way gain or lose financially from the results of this study. The authors have not been employed by such an organization. The authors have not act as an expert witness on the subject of the study. The authors do not have any other competing interest.

References

[1] L. Abela, L. Simmons, K. Steindl, et al., N8-acetylspermidine as a potential plasma biomarker for Snyder-Robinson syndrome identified by clinical metabolomics, J. Inherit. Metab. Dis. 39 (1) (2016) 131–137.

[2] L. Abela, R. Spiegel, L.M. Crowther, et al., Plasma metabolomics reveals a diagnostic metabolic fingerprint for mitochondrial aconitase (ACO2) deficiency, PLoS One 12 (5) (2017).

[3] P.S. Atwal, T.R. Donti, A.L. Cardon, et al., Aromatic L-amino acid decarboxylase deficiency diagnosed by clinical metabolomics profiling of plasma, Mol. Genet. Metab. 115 (2015) 91–94.

[4] H. Blasco, P. Corcia, P.F. Pradat, Metabolomics in cerebrospinal fluid of patients with amyotrophic lateral sclerosis: an untargeted approach via high-resolution mass spectrometry, J. Proteome Res. 12 (8) (2013) 3746–3754.

[5] H. Blasco, L. Nadal-Desbarats, P.F. Pradat, Untargeted 1H-NMR metabolomics in CSF: toward a diagnostic biomarker for motor neuron disease, Neurology 82 (13) (2014) 1167–1174.

[6] E. Cassol, V. Misra, A. Dutta, S. Morgello, D. Gabuzda, Cerebrospinal fluid metabolomics reveals altered waste clearance and accelerated aging in HIV patients with neurocognitive impairment, AIDS 28 (11) (2014) 1579–1591.

[7] K.L.M. Coene, L.A.J. Kluijtmans, E. van der Heeft, Next-generation metabolic screening: targeted and untargeted metabolomics for the diagnosis of inborn errors of metabolism in individual patients, J. Inherit. Metab. Dis. 41 (3) (2018) 337–353.

[8] M.L. Couce, M.D. Bóveda, C. García-Jiménez, Clinical and metabolic findings in patients with methionine adenosyltransferase I/III deficiency detected by newborn screening, Mol. Genet. Metab. 110 (3) (2013) 218–221.

[9] J. Denes, E. Szabo, S.L. Robinette, et al., Metabonomics of newborn screening dried blood spot samples: a novel approach in the screening and diagnostics of inborn errors of metabolism, Anal. Chem. 84 (22) (2012) 10113–10120.

[10] T.R. Donti, G. Cappucio, L. Hubert, et al., Diagnosis of adenylosuccinate lyase deficiency by metabolomic profiling in plasma reveals a phenotypic spectrum, Mol Genet Metab Rep 8 (2016) 61–66.

[11] K.E. Glinton, P.J. Benke, M.A. Lines, et al., Disturbed phospholipid metabolism in serine biosynthesis defects revealed by metabolomics profiling, Mol. Genet. Metab. 123 (2018) 309–316.

[12] H. Gonzalo, L. Brieva, F. Tatzber, Lipidome analysis in multiple sclerosis reveals protein lipoxidative damage as potential pathogenic mechanism, J. Neurochem. 123 (4) (2012) 622–634.

[13] H.A. Haijes, M. Willemsen, M. van der Ham, Direct-infusion based non-quantitative metabolomics identifies metabolic disease in patients' dried blood spots and plasma, Metabolites 9 (2019) 12.

[14] R. Karlíková, K. Micová, L. Najdekr, Metabolic status of CSF distinguishes rats with tauopathy from controls, Alzheimers Res. Ther. 9 (1) (2017) 78.

[15] A.D. Kennedy, K.L. Pappan, T.R. Donti, Elucidation of the complex metabolic profile of cerebrospinal fluid using an untargeted biochemical profiling assay, Mol. Genet. Metab. 121 (2) (2017) 83–90.

[16] S.D. Lamour, V.P. Alibu, A. Holmes, J.M. Sternberg, Metabolic profiling of central nervous system disease in *Trypanosoma brucei rhodesiense* infection, J. Infect. Dis. 216 (10) (2017) 1273–1280.

[17] S. Malvagia, C.A. Haynes, L. Grisotto, Heptadecanoylcarnitine (C17) a novel candidate biomarker for newborn screening of propionic and methylmalonic acidemias, Clin. Chim. Acta 450 (2015) 342–348.

[18] S. Mason, C. Reinecke, R. Solomons, Cerebrospinal fluid amino acid profiling of pediatric cases with tuberculous meningitis, Front. Neurosci. 11 (2017) 534.

[19] M.J. Miller, A.D. Kennedy, A.D. Eckhart, et al., Untargeted metabolomic analysis for the clinical screening of inborn errors of metabolism, J. Inherit. Metab. Dis. 38 (2015) 1029–1039.

[20] M.J. Miller, B.L. Bostwick, A.D. Kennedy, et al., Chronic oral L-carnitine supplementation drives marked plasma TMAO elevations in patients with organic acidemias despite dietary meat restrictions, JIMD Reports 30 (2016) 39–44.

[21] N. Mizutani, C. Hayakawa, Y. Ohya, K. Watanabe, Y. Watanabe, A. Mori, Guanidino compounds in hyperargininaemia, Tohoku J. Exp. Med. 153 (3) (1987) 197–205.

[22] R. Obeid, M. Kasoha, J.P. Knapp, P. Kostopoulos, G. Becker, K. Fassbender, W. Herrmann, Folate and methylation status in relation to phosphorylated tau protein(181P) and beta-amyloid(1-42) in cerebrospinal fluid, Clin. Chem. 53 (6) (2007) 1129–1136.

[23] H. Peretz, D.G. Watson, G. Blackburn, et al., Urine metabolomics reveals novel physiologic functions of human aldehyde oxidase and provides biomarkers for typing xanthinuria, Metabolomics 8 (2012) 951–959.

[24] D. Pieragostino, M. D'Alessandro, M. di Ioia, An integrated metabolomics approach for the research of new cerebrospinal fluid biomarkers of multiple sclerosis, Mol. BioSyst. 11 (6) (2015) 1563–1572.

[25] M. Shichiri, The role of lipid peroxidation in neurological disorders, J. Clin. Biochem. Nutr. 54 (3) (2014) 151–160.

[26] D. Stoessel, C. Schulte, M.C. Teixeira Dos Santos, Promising metabolite profiles in the plasma and CSF of early clinical Parkinson's disease, Front. Aging Neurosci. 10 (2018) 51.

[27] L.W. Sumner, A. Amberg, D. Barrett, et al., Proposed minimum reporting standards for chemical analysis Chemical Analysis Working Group (CAWG) Metabolomics Standards Initiative (MSI), Metabolomics 3 (2007) 211–221.

[28] C.D. van Karnebeek, L. Bonafé, X.Y. Wen, NANS-mediated synthesis of sialic acid is required for brain and skeletal development, Nat. Genet. 48 (7) (2016) 777–784.

[29] L. Venter, Z. Lindeque, P. Jansen van Rensburg, et al., Untargeted urine metabolomics reveals a biosignature for muscle respiratory chain deficiencies, Metabolomics 11 (1) (2015) 111–121.

[30] W.R. Wikoff, J.A. Gangoiti, B.A. Barshop, et al., Metabolomics identifies perturbations in human disorders of propionate metabolism, Clin. Chem. 53 (12) (2007) 2169–2176.

[31] D.S. Wishart, M.J. Lewis, J.A. Morrissey, The human cerebrospinal fluid metabolome, J Chromatogr B Analyt Technol Biomed Life Sci 871 (2) (2008) 164–173.

[32] D.S. Wishart, T. Jewison, A.C. Guo, et al., HMDB 3.0 – the human metabolome database in 2013, Nucleic Acids Res. 41 (2013) 801–807.

[33] M. Yudkoff, Interactions in the metabolism of glutamate and the branched-chain amino acids and ketoacids in the CNS, Neurochem. Res. 42 (2017) 10–18.